

International Journal of Structural Engineering

ISSN online: 1758-7336 - ISSN print: 1758-7328

<https://www.inderscience.com/ijstructe>

Finite element analysis of thermoelastic free vibration behaviour of hardcore higher-order doubly curved sandwich shell panel

Sushmita Dash, Trupti Ranjan Mahapatra, Kulmani Mehar, Isham Panigrahi, Debadutta Mishra

DOI: [10.1504/IJSTRUCTE.2022.10048429](https://doi.org/10.1504/IJSTRUCTE.2022.10048429)

Article History:

Received:	11 May 2022
Accepted:	15 May 2022
Published online:	07 November 2022

Finite element analysis of thermoelastic free vibration behaviour of hardcore higher-order doubly curved sandwich shell panel

Sushmita Dash

School of Mechanical Engineering,
KIIT Deemed to be University,
Bhubaneswar, Odisha 751024, India
Email: gungunsushmita@gmail.com

Trupti Ranjan Mahapatra*

Department of Production Engineering,
Veer Surendra Sai University of Technology (VSSUT),
Burla, Odisha 768018, India
Email: trmahapatra_pe@vssut.ac.in
*Corresponding author

Kulmani Mehar

Department of Mechanical Engineering,
Vignan's Institute of Information Technology, India
Email: kulmanimehar@gmail.com

Isham Panigrahi

School of Mechanical Engineering,
KIIT Deemed to be University,
Bhubaneswar, Odisha 751024, India
Email: ipanigrahifme@kiit.ac.in

Debadutta Mishra

Department of Production Engineering,
Veer Surendra Sai University of Technology (VSSUT),
Burla, Odisha 768018, India
Email: dmvssut@gmail.com

Abstract: Free vibration analysis is carried through for functionally graded material (FGM) sandwich structure under uniform thermal loading and the material property variation according to the power-law distribution. A self-prepared computer code in MATLAB numeric computing environment based on finite element scheme using higher-order kinematics and replicating quadratic function is equipped for the computation of responses for symmetric as well as unsymmetric doubly curved sandwich structure under diverse

support conditions. For numerical approximation while deriving the system of equations, Hamilton's principle is utilised to evaluate the thermo-elastic natural frequencies and the critical buckling temperature. An isoparametric Lagrangian element with zero order Hermitian interpolation function is utilised for model discretisation. After establishing the convergence and validity, the present higher-order model is further hold out for solving diverse numerical illustrations and functional inferences those will assist in designing the imminent graded structures serving under intense thermal loading in high-performance engineering applications.

Keywords: sandwich FGM curved panel; HOSDST; FEM; MATLAB computer code; free vibration analysis; thermal environment.

Reference to this paper should be made as follows: Dash, S., Mahapatra, T.R., Mehar, K., Panigrahi, I. and Mishra, D. (2023) 'Finite element analysis of thermoelastic free vibration behaviour of hardcore higher-order doubly curved sandwich shell panel', *Int. J. Structural Engineering*, Vol. 13, No. 1, pp.80–108.

Biographical notes: Sushmita Dash is currently working as an Assistant Professor in the Department of Mechanical Engineering, GITA Autonomous College Bhubaneswar, India. She is pursuing her PhD in the domination of Numerical Analysis of Functionally Graded Materials and fascinated to implement the same in design/manufacturing works. Her current research includes numerical, simulation and experimental analysis of functionally graded material, smart composite structure, vibro-acoustic analysis, machining and optimisation. She is guiding two MTech students and has received 'Research Excellence Award' 2022 for her journal paper title: 'Finite element solution of stress and flexural strength of functionally graded doubly curved sandwich shell panel' from the Institute of Scholars (INSC).

Trupti Ranjan Mahapatra completed his PhD in the domination of Numerical Analysis of Laminated Composite Structure and fascinated to implement the same in production/manufacturing works. His current research interest includes numerical, simulation and experimental analysis of layered composite structure, smart composite structure, functionally graded material, vibro-acoustic analysis, machining and optimisation. He has guided two PhD scholars and currently guiding five scholars, and has received few national and international awards including the prestigious 'IEI Young Engineers Award 2016–2017' from the Institute of Engineers (IE), India, handled few sponsored projects received from Department of Science and Technology (DST), Government of India and TEQIP.

Kulmani Mehar is currently working in the Department of Mechanical Engineering, Vignan's Institute of Information Technology, India. His research interest includes CNT, smart material, composite material, mechanisms synthesis, numerical and experimental analysis. He has more than 50 publications to his credit in various international journals of repute.

Isham Panigrahi is an Associate Professor and Deputy Director on the KIIT Student Research Centre at KIIT Deemed to be University. His career is spanning for 20 years in teaching, consulting, skill training and placements, new product design and prototyping and research in mechanical engineering and automobile engineering. He has ten years of hands on experience in building ATV, formula-one cars, electric and solar cars, motorised and solar boats. Presently, he is involve in many innovative projects works in area of

automotive, aeronautics, electric and solar vehicles, marine applications, robotics, machine condition monitoring, FEA, NVH and composite materials and new products prototyping.

Debadutta Mishra has completed his PhD in the area of Robotics. He extended his contribution the domain of machining, welding, composite materials, smart materials, production planning and optimisation. He has guided six PhD scholars and eight doctoral scholars are continuing under his supervision. He has also handled few sponsored projects received AICTE, Government of India and TEQIP. Five patents have been published to his credit.

1 Introduction

Functionally graded materials (FGMs) are prepared by continuous and smooth variations in their characteristics through the dimensions that benefits to overcome the drawback of delamination associated with laminated composite structure under extreme thermal loading. Usually, these novel materials are made by the combination of ceramic and metals which possess the ability to resist high temperatures without changing any of its structural behaviour. There exist variations in material properties such as the elastic moduli and the density throughout the thickness and it is governed by the material homogenisation law between the metal and the ceramic phases. Moreover, hardcore sandwich FGM structures have the advantage of possessing graded properties at every single point in various dimensions that leads to their ability to develop ultra-high temperature resistant property and ultimately, makes them functional in high performance spacecraft, civil and engineering applications in need of weight sensitive structure under extreme environmental conditions. Therefore, the detail knowledge of the structural behaviour and precise prophecy of mechanical responses is very much indispensable for their distinguished structural design and to rationalise their apposite operation. Amidst other mechanical responses, the first mode natural frequency is a crucial element in the analysis of any structure or structural component specifically when the structure is subjected to large amplitude vibration in hostile environment. Therefore, the precise estimation of the fundamental frequency is important to avoid resonance and subsequent damage or failure of the structure. Also, the influence of temperature that imparts residual stresses along with other design parameters of the hardcore sandwich FGM structure has been the quest for the researchers. In order to address this issue, numerical and/or experimental analysis pertaining to the fundamental frequency of vibration of these structures has become an emerging theme for the research community. Furthermore, the influence of temperature on these parameters has also become the quest for the researchers and number of works is being done in this domain.

The numerical as well as analytical studies have been carried out to study the bending, buckling and free vibration characteristics of FGM structure by using the basic classical laminate theory (CPT) (Phu et al., 2021), the first-order shear deformation plate theory (FSDPT) (Ziou et al., 2016), three-dimensional (3D) analysis (Li et al., 2008), third-order shear deformation plate theories (TSDTs) (Aghababaei and Reddy, 2009), higher-order shear deformation shell theory (HOSDST) (Srividhya et al., 2019) and other refined theories (Mouffoki et al., 2019) based on equivalent single layer theories. Eight-nodded higher-order quadrilateral plate element with 104 degrees of freedom

(DOF) has been utilised by Natarajan and Manickam (2012) for accurate prediction of the flexural and free vibration behaviour of FGM plates. The free vibration behaviour of hard and soft-core sandwich FGM plates have also been analysed by improved high-order sandwich plate theory (Khalili and Mohammadi, 2012) in thermal environment. The HOSDST is also utilised by Zenkour (2013) to study the flexural behaviour of sandwich FGM plates by considering the effect of shear strains and transverse normal strain. Pandey and Pradyumna (2015) developed a layer wise finite element (FE) formulation based on the FSDPT and reported the free vibration responses of functionally graded material sandwich (FGMS) shells under thermal environment by employing an eight-noded isoparametric element with nine DOF per node. Researchers also made efforts to eliminate the use of shear correction factors by implementing refined theories those account for sinusoidal, parabolic, hyperbolic, and exponential distributions of transverse shear strains while studying the vibration characteristics of temperature dependent FGM plates (Attia et al., 2015). Optimised unified hyperbolic displacement field based on Carrera's unified formulation (CUF) (Mantari and Monge, 2016), three unknown non-polynomial shear deformation theory (Tounsi et al., 2016) and FE formulation based on higher-order layer wise theory (Pandey and Pradyumna, 2017) and the FSDPT (Joseph and Mohanty, 2019) were proposed for studying the vibration behaviour of temperature independent as well as temperature dependent sandwich FGM plates. Moreover, relative study on the buckling, bending and vibration of nano-sandwich plates based on the CPT, FSDPT, sinusoidal shear deformation theory (SSDT) and refined zigzag theory (RZT) revealed that the RZT is more accurate in predicting the responses without necessitating any shear correction factors (Kolahchi, 2017). A refined quasi-3D shear deformation theory (four unknown) (Mahmoudi et al., 2019) is also implemented to investigate the thermo mechanical behaviour of sandwich FGM plates. Mahapatra et al. (2017) projected the inevitability of the HOSDST during the numerical analysis of the FGM structure in thermal environment. The vibration characteristics under thermal environment for porous FGM structure is also investigated (Gupta and Talha, 2018) using four unknown non-polynomial based on HSDPT and normal deformation theory utilising a C0 continuous FE having eight DOF at each node. The effect of shear deformation is also incorporated by the use of non-local n th order HSDPT (Berghouti et al., 2019), which is devoid of the shear correction factors, to study the dynamic behaviour of FGM porous nanobeams. The static and dynamic responses of beams have been accurately computed analytically (Chaabane et al., 2019) by using a hyperbolic shear deformation theory (HOSDT) and considering the property variation according to exponential and power-law distributions. The buckling behaviour of FGM nanoplates (Karami et al., 2019a) and doubly curved shells (Karami et al., 2019b) have been studied analytically in the framework of the HOSDT and using variational approach for deriving the governing equation. Formulations based on Reddy's TSDT and Hamilton's principle including thermal effects is also reported (Daikh, 2019) for the exact solution of thermoelastic natural frequencies of simply supported FGMS plates. 3D graded FE using commercial software (ABAQUS) is implemented (Burlayenko et al., 2019) to accurately compute thermoelastic natural frequencies of FGMS plates. In order to make the formulation computationally faster to solve, past researchers attempted to reduce the number of unknowns (3 or 4) (Rahmani et al., 2020; Belarbi et al., 2021) in the displacement field with needless of any shear correction factor for the free vibration, bending and buckling behaviour of graded sandwich plates. Computationally efficient (without requiring shear correction factors and free of shear locking) higher-order refined

layer wise FEM considering the HOSDST for the core and the FSDPT for the face sheets and sustaining a continuity of displacement at layers has been proposed (Hirane et al., 2021) for investigating the deflection and natural frequencies of FGMS plates. Unlike the conventional layer wise models, here the number of unknowns does not increase with increasing number of layers. The necessity of the non-local parameters is incorporated via a modified kind of the classical non-local elasticity theory (Vinh and Tounsi, 2021) to take into account for through the thickness material variation in free vibration of sandwich FGM nanoplates. From the open literature available it is precipitated that though numerous amounts of numerical/analytical research work have been carried out regarding the buckling, bending and free vibration of sandwich FGM panels with/without considering the thermal effect, most of the studies focus majorly on the sandwich FGM plates. Very few pieces of studies are existing on the free vibration analysis of sandwich FGM structure taking the curvatures (spherical, cylindrical, elliptical, hyperboloid) on both sides into consideration. Moreover, limited number of studies is available foregrounding the implementation of the HOSDST kinematics in combination with FE to examine the natural frequency of sandwich FGM doubly curved panels in thermal environment. Thus, free vibration analysis of sandwich FGM doubly curved shell structure requires a deep insight.

In this numerical work, the free vibration behaviour of sandwich FGM doubly curved shell panels with diverse types of shell geometries (flat, hyperboloid, elliptical, spherical, and cylindrical panel) subjected to thermal environment is investigated. The power-law is used for governing the material homogenisation in terms of the volume fractions of the individual constituents for attaining gradual variation of ceramic at the interface into pure metal at the surface. A second order complete FEM scheme has been developed and implemented in this research. The mathematical formulation is derived using the Reddy's HOSDST type of strain-displacement kinematics which has been established to be a more realistic approximation of the shear deformable structural behaviour. The incorporation of the higher-order terms in the formulation and implementation of isoparametric Lagrangian element with zero order Hermitian interpolation function (81 DOF per element) ensures to apprehend the exact structural behaviour under extreme environment condition. The convergence behaviour as well as the validity of the proposed scheme with those of the other 2D analytical/numerical models and 3D elasticity solutions is established by considering various parameters. Subsequently, numerical results are provided to investigate the influence of various design factors (FGMS symmetry type, aspect ratio, curvature ratio, thickness ratio, power-law index, and support conditions) on the natural frequency of FGMS curved panel structures followed by few useful concluding remarks.

2 FE formulation

For the computation of the free vibration responses of hard core FGMS single/doubly curved shell panels, a general mathematical formulation is derived. The top and bottom faces of the shell panel are made up of FGM layers with pure ceramic phase at the core and the face sheets have material graded as metal at the surface into ceramic at the interface. The variation of individual constituents along the thickness direction is assumed to be according to the power-law and the structural properties such as the

density, elastic moduli and Poisson's ratio vary obeying the following relation (Zenkour, 2005):

$$P(z) = P_m + (P_c - P_m)V_f^{(n)} \quad (1)$$

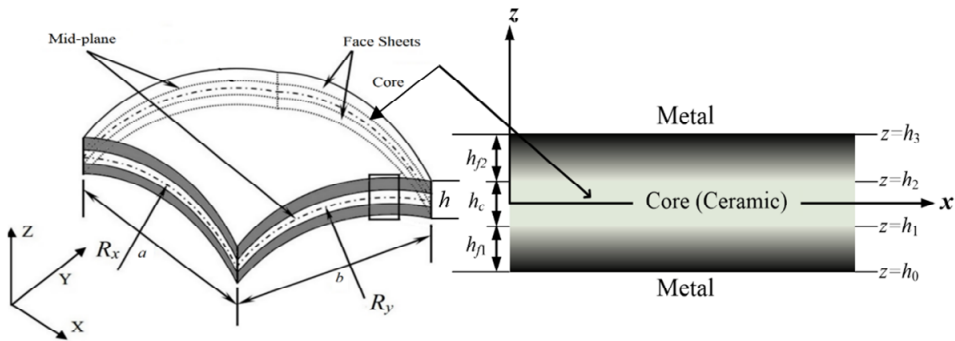
where P_m is the material properties of metal and P_c is the material properties of ceramic. The volume fraction of the ceramic ($V_f^{(n)}$, $n = 1, 2, 3$) varies through the thickness following the power-law (Zenkour, 2005) as:

$$V_f^{(1)} = \left(\frac{z - h_0}{h_1 - h_0} \right)^k, \quad z \in [h_0, h_1];$$

$$V_f^{(2)} = 1z \in [h_1, h_2]; \quad V_f^{(3)} = \left(\frac{z - h_3}{h_2 - h_3} \right)^k, \quad z \in [h_2, h_3] \quad (2)$$

The thickness coordinate (z) has different levels (h_0 , h_1 , h_2 and h_3) as shown in the schematic figure of the geometry of the sandwich FGM shell panel as illustrated in Figure 1.

Figure 1 Geometry and thickness coordinate levels in hard core sandwich FGM structure



The present FGMS curved panel model is assumed to be made up of three layers, i.e., one isotropic core layer (made of pure ceramic phase) bounded by two FGM face-sheets. If the different layers of the sandwich structure are assumed to be perfectly bonded with each other and do not distort due to deformation. The mid-plane of the geometry is considered as the reference plane to evaluate the mechanical responses. The projection of the sandwich shell panel with dimensions ($a \times b \times h$) on the XY plane is a rectangular shape with length a and width b . Here, h is the total thickness of the sandwich shell panel, h_c is the thickness of the core, h_{f1} is the thickness of the bottom face sheet and h_{f2} is the thickness of the top face sheet such that $h = h_c + h_{f1} + h_{f2}$; $h_c = h_2 - h_1$; $h_{f1} = h_3 - h_2$ and $h_{f2} = h_1 - h_0$. R_x and R_y are the principal radius of curvature along x and y direction, respectively and the twist radius of curvature is R_{xy} defined at the mid-plane ($z = 0$). Further, various types of the shallow single and doubly curved shell geometries are achieved by changing the curvature configurations, i.e., flat ($R_x = R_y = \infty$), cylindrical ($R_x = R$, $R_y = \infty$), spherical ($R_x = R$, $R_y = R$), elliptical ($R_x = R$, $R_y = 2R$) and hyperboloid ($R_x = R$, $R_y = -R$), where R is a constant.

In the present study, the displacement field of the sandwich FGM structure has been modelled employing the HOSDST type mid-plane kinematic. The global displacement component (u_x , u_y and u_z) of any point in the sandwich shell panel are expressed as the polynomial function of nine unknown parameters (u_{x0} , u_{y0} , u_{z0} , φ_x , φ_y , ψ_x , ψ_y , θ_x and θ_y) (Kant and Swaminathan, 2002). The displacement u_x , u_y and u_z along X , Y and Z -axis, respectively are expressed using Taylor’s series respecting the thickness coordinate as (Mahapatra et al., 2017):

$$\left. \begin{aligned} u_x &= u_{x0}(x, y, t) + z\varphi_x(x, y, t) + z^2\psi_x(x, y, t) + z^3\theta_x(x, y, t) \\ u_y &= u_{y0}(x, y, t) + z\varphi_y(x, y, t) + z^2\psi_y(x, y, t) + z^3\theta_y(x, y, t) \\ u_z &= u_{z0}(x, y, t) \end{aligned} \right\} \quad (3)$$

where u_x , u_y and u_z are the mid-plane displacements along X , Y and Z -directions, respectively. The variables φ_x and φ_y represent the rotation of transverse normal about the Y and X -axis and ψ_x , ψ_y , θ_x and θ_y are the higher-order terms of the expansion of Taylor’s series at mid-plane of the sandwich panel. All nine unknown parameters are defined at

the mid-plane ($z = 0$), as $u_{x0} = u_x$, $u_{y0} = u_y$, $u_{z0} = u_z$, $\varphi_x = \frac{\partial u_x}{\partial z}$, $\varphi_y = \frac{\partial u_y}{\partial z}$, $\psi_x = \frac{1}{2} \left(\frac{\partial^2 u_x}{\partial z^2} \right)$, $\psi_y = \frac{1}{2} \left(\frac{\partial^2 u_y}{\partial z^2} \right)$, $\theta_x = \frac{1}{6} \left(\frac{\partial^3 u_x}{\partial z^3} \right)$ and $\theta_y = \frac{1}{6} \left(\frac{\partial^3 u_y}{\partial z^3} \right)$.

Equation (3) can be rewritten in terms of the displacement vector of any point within the composite $\{\lambda\} = \{u_x \ u_y \ u_z\}^T$ in the matrix form as:

$$\{\lambda\} = [H_1] \{\lambda_0\} \quad (4)$$

where $\{\lambda_0\} = \{u_{x0} \ u_{y0} \ u_{z0} \ \varphi_x \ \varphi_y \ \psi_x \ \psi_y \ \theta_x \ \theta_y\}$ and $[H_1]$ are the displacement vector at $z = 0$ and thickness coordinate matrix, respectively. The details of $[H_1]$ can be seen in Mahapatra et al. (2017).

Now, the strain tensor is given by:

$$\left. \begin{aligned} \{\varepsilon\} &= \{\varepsilon_{xx} \ \varepsilon_{yy} \ \varepsilon_{xy} \ \varepsilon_{xz} \ \varepsilon_{yz}\}^T \\ &= \left\{ \left(\overline{u_x} \right)_{,x} + \frac{\overline{u_z}}{R_x} \right\} \left\{ \left(\overline{u_y} \right)_{,y} + \frac{\overline{u_z}}{R_y} \right\} \left\{ \left(\overline{u_x} \right)_{,y} + \left(\overline{u_y} \right)_{,x} + \frac{2\overline{u_z}}{R_{xy}} \right\} \left\{ \left(\overline{u_x} \right)_{,z} + \left(\overline{u_z} \right)_{,x} - \frac{\overline{u_x}}{R_x} \right\} \dots \\ &\dots \left\{ \left(\overline{u_y} \right)_{,z} + \left(\overline{u_z} \right)_{,y} - \frac{\overline{u_y}}{R_y} \right\}^T \end{aligned} \right\} \quad (5)$$

The in-plane strain displacement vector can be expressed by using equation (3) in equation (5), as:

$$\{\varepsilon\} = \begin{Bmatrix} \varepsilon_x^0 \\ \varepsilon_y^0 \\ \varepsilon_{xy}^0 \\ \varepsilon_{xz}^0 \\ \varepsilon_{yz}^0 \end{Bmatrix} + z \begin{Bmatrix} k_x^1 \\ k_{xy}^1 \\ k_{xz}^1 \\ k_{yz}^1 \end{Bmatrix} + z^2 \begin{Bmatrix} k_x^2 \\ k_{xy}^2 \\ k_{xz}^2 \\ k_{yz}^2 \end{Bmatrix} + z^3 \begin{Bmatrix} k_x^3 \\ k_{xy}^3 \\ k_{xz}^3 \\ k_{yz}^3 \end{Bmatrix} = [H_2] \{\bar{\varepsilon}\} \quad (6)$$

where $[H_2]$ and $\{\bar{\varepsilon}\}$ are the thickness coordinate matrix (function of z coordinate) and mid-plane strain vector (function of x and y), respectively such that the bending, curvature, and the higher-order terms are denoted by the superscripts 0, 1, 2, 3 and expressed as:

$$\{\bar{\varepsilon}\} = \begin{Bmatrix} \varepsilon_1^0 & \varepsilon_2^0 & \varepsilon_6^0 & \varepsilon_5^0 & \varepsilon_4^0 & \kappa_1^1 & \kappa_2^1 & \kappa_6^1 & \kappa_5^1 & \kappa_4^1 \\ \kappa_1^2 & \kappa_2^2 & \kappa_6^2 & \kappa_5^2 & \kappa_4^2 & \kappa_1^3 & \kappa_2^3 & \kappa_6^3 & \kappa_5^3 & \kappa_4^3 \end{Bmatrix}^T \quad (7)$$

In this present investigation, the sandwich FGM curved panel is considered to be under uniform temperature loading which is assumed to be distributed uniformly through the thickness of the shell structure as well as over the entire surface and that remain unaltered. Thus, the uniform change in temperature (ΔT) of the structure in terms of the initial temperature (T_i) and the final temperature (T_f) is given by $\Delta T = (T_f - T_i)$.

Now, the thermoelastic constitutive relations of the pre-stressed (due to a uniform thermal loading) doubly curved hard core sandwich structure for the generalised stress tensor can be written as:

$$\{\tilde{\sigma}_{ij}\}^k = [\bar{\Theta}_{ij}]^k \{\varepsilon_{ij} - \alpha_{ij} \Delta T\}^k \quad (8)$$

where $\{\tilde{\sigma}_{ij}\}^k = \{\tilde{\sigma}_1 \quad \tilde{\sigma}_2 \quad \tilde{\sigma}_6 \quad \tilde{\sigma}_5 \quad \tilde{\sigma}_4\}^T$ and $\{\varepsilon_{ij}\}^k = \{\varepsilon_1 \quad \varepsilon_2 \quad \varepsilon_6 \quad \varepsilon_5 \quad \varepsilon_4\}$ are the stress and corresponding strain vector, respectively. $\{\alpha_{ij}\}^k = \{\alpha_1 \quad \alpha_2 \quad 2\alpha_{12}\}^T$ is the thermal expansion coefficient vector. $[\bar{\Theta}_{ij}]^k$ is the transferred reduced elastic constant/reduced stiffness matrix and k being the layer number (1 for the bottom face, 2 for the core layer and 3 for the top face).

So, equation (7) can now be rewritten as:

$$\{\tilde{\sigma}_{ij}\}^k = \begin{bmatrix} \bar{\Theta}_{11} & \bar{\Theta}_{12} & \bar{\Theta}_{16} & 0 & 0 \\ \bar{\Theta}_{21} & \bar{\Theta}_{22} & \bar{\Theta}_{26} & 0 & 0 \\ \bar{\Theta}_{16} & \bar{\Theta}_{26} & \bar{\Theta}_{66} & 0 & 0 \\ 0 & 0 & 0 & \bar{\Theta}_{55} & \bar{\Theta}_{54} \\ 0 & 0 & 0 & \bar{\Theta}_{45} & \bar{\Theta}_{44} \end{bmatrix}^k \left[\begin{array}{c} \left\{ \varepsilon_1 \right\}^k \\ \left\{ \varepsilon_2 \right\}^k \\ \left\{ \varepsilon_6 \right\}^k \\ \left\{ \varepsilon_5 \right\}^k \\ \left\{ \varepsilon_4 \right\}^k \end{array} - \begin{array}{c} \left\{ \alpha_1 \right\}^k \\ \left\{ \alpha_2 \right\}^k \\ \left\{ 2\alpha_{12} \right\}^k \\ 0 \\ 0 \end{array} \right] \Delta T \quad (9)$$

The in-plane thermal forces induced due to the uniform temperature load can be derived by the integration of the stress equation over the panel thickness and conceded as:

$$\left[\{\tilde{N}_{\Delta T}\} \quad \{\tilde{M}_{\Delta T}\} \quad \{\tilde{\Pi}_{\Delta T}\} \right] = \left[\sum_{k=1}^N \int_{z_{k-1}}^{z_k} \left\{ [\bar{\Theta}]^k \left\{ \{\alpha\}^k (1, z, z^3) \Delta T \right\} \right\} dz \right] \quad (10)$$

The details for the resultant compressive in-plane thermal force vector, the moment vector, i.e., $\{\tilde{N}_{\Delta T}\} = [(\tilde{N}_{\Delta T})_1 \quad (\tilde{N}_{\Delta T})_2 \quad (\tilde{N}_{\Delta T})_{12}]^T$ and $\{\tilde{M}_{\Delta T}\} = [(\tilde{M}_{\Delta T})_1 \quad (\tilde{M}_{\Delta T})_2 \quad (\tilde{M}_{\Delta T})_{12}]^T$ as well as the higher-order terms $\{\tilde{\Pi}_{\Delta T}\} = [(\tilde{\Pi}_{\Delta T})_1 \quad (\tilde{\Pi}_{\Delta T})_2 \quad (\tilde{\Pi}_{\Delta T})_{12}]^T$ can be seen in Mahapatra et al. (2017). Now, the corresponding work done on the sandwich FGM shell panel by the in-plane thermal force $\{\tilde{N}_{\Delta T}\}$ is given by:

$$\begin{aligned}
 \{W_T\} = & \int_v \frac{1}{2} \left[\left[\left\{ \frac{\partial(\bar{u}_x)}{\partial x} \right\}^2 + \left\{ \frac{\partial(\bar{u}_y)}{\partial x} \right\}^2 + \left\{ \frac{\partial(\bar{u}_z)}{\partial x} \right\}^2 \right] \{N_{\Delta T}\}_1 \right. \\
 & + \left. \left[\left\{ \frac{\partial(\bar{u}_x)}{\partial y} \right\}^2 + \left\{ \frac{\partial(\bar{u}_y)}{\partial y} \right\}^2 + \left\{ \frac{\partial(\bar{u}_z)}{\partial y} \right\}^2 \right] \{N_{\Delta T}\}_2 \right. \\
 & \left. + 2 \left[\left\{ \frac{\partial(\bar{u}_x)}{\partial x} \right\} \left\{ \frac{\partial(\bar{u}_x)}{\partial y} \right\} + \left\{ \frac{\partial(\bar{u}_y)}{\partial x} \right\} \left\{ \frac{\partial(\bar{u}_y)}{\partial y} \right\} + \left\{ \frac{\partial(\bar{u}_z)}{\partial x} \right\} \left\{ \frac{\partial(\bar{u}_z)}{\partial y} \right\} \right] \{N_{\Delta T}\}_{12} \right] dV
 \end{aligned} \tag{11}$$

Now, incorporating the geometrical distortion due to the thermal loading and rearranging equation (11) in terms of the geometric strain vector $\{\varepsilon_G\}$ and material property matrix $[\Lambda_G]$ by following the steps as derived in Cook et al. (2007), and Mahapatra et al. (2015), the work done expression is given by:

$$\{W_T\} = \frac{1}{2} \int_A \{\varepsilon_G\}^T [\Lambda_G] \{\varepsilon_G\} dA \tag{12}$$

Then, to derive the expression for the kinetic energy (KE) of the vibrating doubly curved sandwich FGM shell panel, the global displacement field vector [equation (1)] expressed with regard to the displacement vector at any point in the mid-plane ($\{\delta\}$) as in equation (4) is utilised.

The general expression for KE of the three-layered sandwich FGM curved panel is given by

$$E_K = \frac{1}{2} \iint \left\{ \sum_{k=1}^3 \int_{z_{k-1}}^{z_k} \rho \{\dot{\lambda}\}^T \{\dot{\lambda}\} dz \right\} dx dy \tag{13}$$

where ρ and $\{\dot{\lambda}\}$ are the mass density and the first-order time-derivative (global velocity vector) of the k^{th} layer, respectively.

Now, by means of equation (4) in equation (13), the KE expression becomes

$$E_K = \frac{1}{2} \int_A \left\{ \sum_{k=1}^3 \int_{z_{k-1}}^{z_k} \{\dot{\lambda}_0\}^T [H_1]^T (\rho)^k [H_1] \{\dot{\lambda}_0\} dz \right\} dA = \frac{1}{2} \int_A \{\dot{\lambda}_0\}^T [m]^k \{\dot{\lambda}_0\} dA \tag{14}$$

where $[m]^k = \sum_{k=1}^3 \int_{z_{k-1}}^{z_k} [H_1]^T \rho^k [H_1] dz$ is the inertia matrix.

The total strain energy (U_T) of the sandwich FGM shell panel is given by:

$$U_\varepsilon = \frac{1}{2} \int_v \{\varepsilon\}^T \{\sigma\} dV = \frac{1}{2} \iint \left\{ \sum_{k=1}^3 \int_{z_{k-1}}^{z_k} \{\varepsilon\}_i^T \{\tilde{\sigma}_i\} dz \right\} dx dy \tag{15}$$

Further substituting equation (5), the expression becomes

$$\begin{aligned}
 U_\varepsilon &= \frac{1}{2} \iint \left\{ \sum_{k=1}^3 \int_{z_{k-1}}^{z_k} \{\varepsilon\}_i^T [\bar{\Theta}] \{\varepsilon_i - \alpha_i \Delta T\} dz \right\} dx dy \\
 &= \frac{1}{2} \iiint \{\varepsilon\}_i^T [\bar{\Theta}] \{\varepsilon\}_i dx dy dz - \frac{1}{2} \iint \left\{ \sum_{k=1}^3 \int_{z_{k-1}}^{z_k} \{\varepsilon\}_i^T [\bar{\Theta}] \{\alpha_i \Delta T\} dz \right\} dx dy
 \end{aligned} \tag{16}$$

Then, using the strain tensor [equation (6)] and the in-plane thermal force [equation (10)] expressions, equation (16) is modified as:

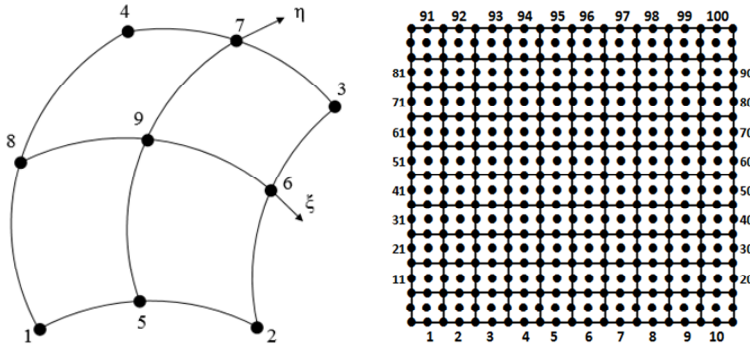
$$U_\varepsilon = \frac{1}{2} \int_A \left(\{\varepsilon\}_i^T [\Lambda_1] \{\varepsilon\}_i \right) dA - \frac{1}{2} \left\{ \sum_{k=1}^3 \int_{z_{k-1}}^{z_k} \{\varepsilon\}_i^T [\bar{\Theta}] \{\alpha_i \Delta T\} dz \right\} dx dy \tag{17}$$

where

$$[\Lambda_1] = \sum_{k=1}^3 \int_{z_{k-1}}^{z_k} [H_1]^T [\bar{\Theta}] [H_1] dz.$$

Now the FEM, which is very well known as a versatile tool for the computation of approximate solutions of numerically tough problems, is implemented for the further analysis purpose. In order to do so, a quadrilateral isoparametric Lagrangian element, that can replicate full quadratic interpolation functions having nine nodes with nine DOF associated with each node ($u_{x0}, u_{y0}, u_{z0}, \varphi_x, \varphi_y, \psi_x, \psi_y, \theta_x, \theta_y$) has been utilised for modelling and discretisation purpose. The details of the element used is represented Figure 2 in the natural coordinate system and the details of the shape functions at different nodes of the element can be seen in Cook et al. (2007), and Mahapatra et al. (2015).

Figure 2 Details of the element used for discretisation and FE mesh



The present assumed displacement field ($\{\lambda_0\}$) in terms of the nodal displacement vector of each node ($\{\lambda_{0i}\} = [u_{x0i} \ u_{z0i} \ \varphi_{xi} \ \varphi_{yi} \ \psi_{xi} \ \psi_{yi} \ \theta_{xi} \ \theta_{yi}]^T$) and the shape function of the i^{th} node (N_i) is expressed as:

$$\{\lambda_0\} = \sum_{i=1}^9 N_i \{\lambda_{0i}\} \tag{18}$$

Now, the mid-plane strain vector with regard to the displacement field vector corresponding to each node of the element can be written as:

$$\{\bar{\varepsilon}\} = [B]\{\lambda_{0i}\} \quad (19)$$

where, $[B]$ is the strain displacement relation matrix in the form of product of shape functions in the strain terms and differential operators.

Now, substituting equation (19) in equation (17), the elemental form of strain energy is expressed as:

$$U_{\varepsilon E} = \frac{1}{2} \int_A \left(\{\lambda_{0i}\}_i^T [B]_i^T [\Lambda_1] [B]_i \{\lambda_{0i}\}_i \right) dA - \{\Xi_{\Delta T}\}_i \quad (20)$$

where $\{\Xi_{\Delta T}\}_i = \frac{1}{2} \int_A \{\lambda_{0i}\}_i^T [B]_i^T \{\tilde{N}_{\Delta T}\} dA$ is the strain energy due to in-plane thermal load vector as a result of uniform temperature change.

Similarly, the elemental work done under the influence of uniform temperature loading can be written by substituting equation (19) into equation (12) as:

$$\{W_{TE}\} = \frac{1}{2} \int_A \left(\{\lambda_{0i}\}_i^T [B]_i^T [\Lambda_G] [B]_i \{\lambda_{0i}\}_i \right) dA \quad (21)$$

The elemental form of KE of the doubly curved sandwich FGM shell panel can be derived by using equation (18) into equation (14) as:

$$\left. \begin{aligned} E_{KE} &= \frac{1}{2} \iint \{\dot{\lambda}_{0i}\}^T [m]^k \{\dot{\lambda}_{0i}\} dx dy \\ &= \frac{1}{2} \int_{-1}^1 \int_{-1}^1 \left((N_i \{\lambda_{0i}\})^T [m]^k (N_i \{\lambda_{0i}\}) \right) |J| d\zeta d\eta \\ &= \frac{1}{2} \int_{-1}^1 \int_{-1}^1 \left(\{\lambda_{0i}\}^T (N_i)^T [m]^k (N_i) \{\lambda_{0i}\} \right) |J| d\zeta d\eta = \frac{1}{2} \{\dot{\lambda}_{0i}\}^T [M]_e \{\dot{\lambda}_{0i}\} \end{aligned} \right\} \quad (22)$$

where $[M]_e$ is the elemental mass matrix at i^{th} node and expressed as

$$[M]_e = \int_{-1}^1 \int_{-1}^1 [N]^T [m] [N] |J| d\zeta d\eta.$$

The weak form of the system governing differential equation meant for the free vibration as well as the buckling analysis of the present sandwich FGM doubly curved shell panel is established by using the variational principle and derived as:

$$\int_{t_1}^{t_2} E dt = 0 \Rightarrow \int_{t_1}^{t_2} [E_{KE} - (W_{TE} + U_{\varepsilon E})] dt = 0 \quad (23)$$

Upon employing the equation for the KE [equation (22)], work done [equation (21)], and strain energy [equation (20)] in equation (23) and incorporating the elemental stiffness

($[K]_e$) and elemental mass ($[M]_e$) matrices, the final equilibrium governing equation can be rearranged as:

$$[K]_e \{\lambda_0\} + [M]_e \{\ddot{\lambda}_0\} = \{F_T\}_e \quad (24)$$

The above equation can be extended to the global form as:

$$[K]\{\lambda_0\} + [M]\{\ddot{\lambda}_0\} = \{F_T\} \quad (25)$$

where $[K]$ is the global stiffness matrix, $\{F_T\}$ is the global thermal load vector of the system and $[M]$ is the global mass matrix.

Now, in order to have the form of the eigenvalue equation, equation (25) is modified and rearranged by introducing the global geometry stiffness matrix ($[K_G]$) that includes the effects due to the thermal load so as to drop the thermal load term and conceded as:

$$[[K] - [K_G] - \omega_n^2 [M]]\{\Delta\} = 0 \quad (26)$$

where ω_n and Δ are the natural frequency (eigenvalue) and the corresponding eigenvector, respectively.

In order to select the temperature range for the present analysis so that buckling of the structure does not occur under uniform thermal load while computing the thermoelastic free vibration responses, the buckling analysis is first performed. The equilibrium equation for the buckling analysis of the sandwich FGM shell panel in the form of eigenvalue and eigenvector is expressed by means of the global stiffness matrix $[K]$ and global geometry stiffness matrix $[K_G]$ as:

$$([K] - \gamma_{icr} [K_G])\{\zeta_i\} = 0 \quad (27)$$

The value of the critical buckling temperature (T_{cr}) is computed as the product of the minimum value of the i^{th} eigenvalue ($\gamma_{icr|_{\min}}$) the corresponding eigenvector (ζ_i) and temperature rise ΔT .

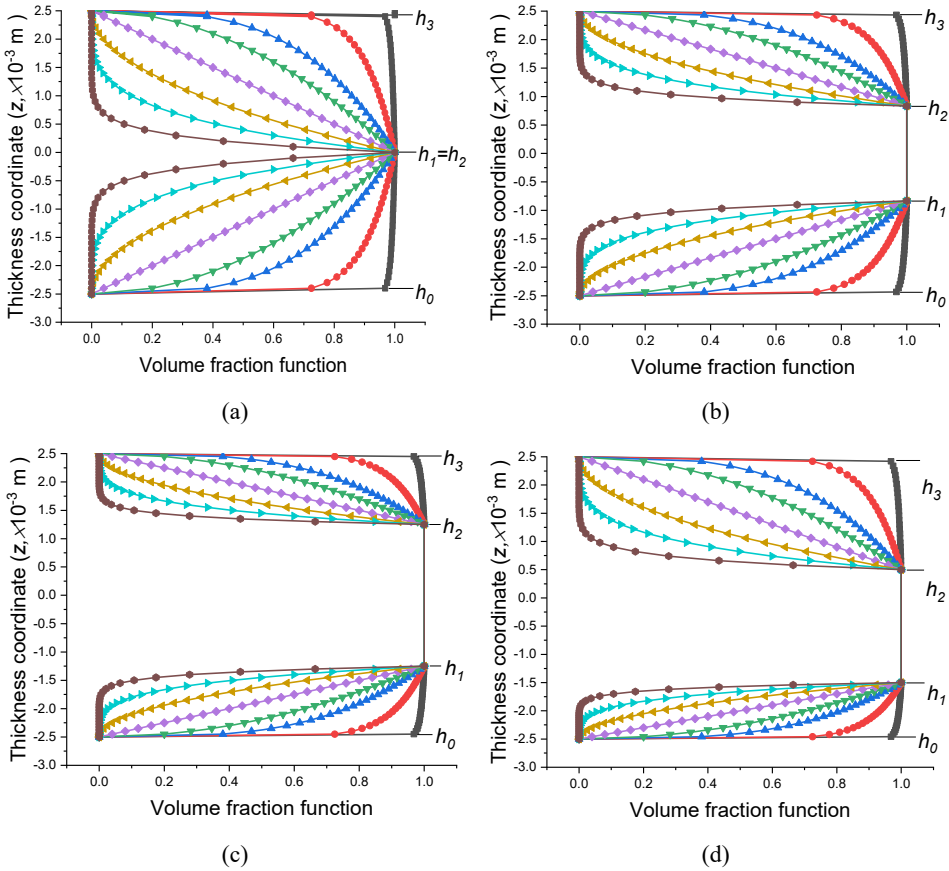
Firstly, the elemental matrices (mass and stiffness) are evaluated using the currently proposed FE steps. Then, the corresponding global matrices are derived by assembling the elemental matrices. Prior to solving equation (26) to compute the natural frequencies, equation (27) is first solved to suitably select the range of temperature to be selected for analysis avoiding buckling of the structure under thermal load. Finally, the desired responses are computed by solving the system governing equation.

3 Results and discussion

Now, the free vibration characteristic of sandwich FGM single/doubly curved (flat, spherical, cylindrical, elliptical and hyperboloid) structure subjected to uniform temperature loading is investigated using the proposed HOSDST-based FE scheme. Personalised MATLAB computer code is prepared for the implementation of the present FE model and computation of the responses. The structure is considered to be a hard code sandwich FGM shell panel with the core made up of either alumina (Al_2O_3) or zirconia (ZrO_2) ceramic and the surface of aluminium (Al) metal with the constituents varying from ceramic at the interface to metal at the surface. The following materials properties as mentioned in Table 1 have been utilised throughout the analysis excepting those are

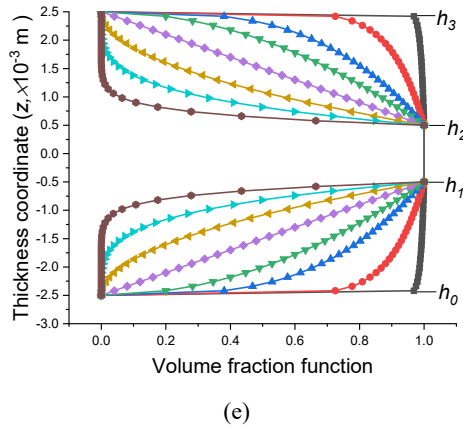
stated differently. The configuration of the sandwich FGM panel symmetry is defined in respect of the ratio of the core thickness (h_c) and the face thicknesses [bottom face (h_{f1}) and top face (h_{f2})] as mentioned in Table 2. The various symmetry schemes of the sandwich FGM shell panel considered in the present study are also outlined in Figure 3. The panels are assumed to have power-law index $k = 2$, thickness $h = 0.005$ m with the length and width determined as per the specified values of thickness ratio (a/h) and aspect ratio (a/b) which are considered as 10 and 1, respectively if not stated explicitly. The non-dimensional form of the fundamental frequencies are expressed as $\varpi = \omega a^2(\rho_f / E_{2,f}) / h$.

Figure 3 Details of the distinction of volume fraction according to power-law indexes through the thickness (a) 1-0-1, (b) 1-1-1, (c) 1-2-1, (d) 1-2-2, and (e) 2-1-2 sandwich FGM panel (see online version for colours)



- Notes: \blacksquare $k = 0.01$, \bullet $k = 1.0$, \blacktriangle $k = 0.3$, \blacktriangledown $k = 0.5$, \blacklozenge $k = 1.0$,
 \blacktriangleright $k = 2.0$, \blacktriangleleft $k = 4.0$, \bullet $k = 10.0$.

Figure 3 Details of the distinction of volume fraction according to power-law indexes through the thickness (a) 1-0-1, (b) 1-1-1, (c) 1-2-1, (d) 1-2-2, and (e) 2-1-2 sandwich FGM panel (continued) (see online version for colours)



Notes: \blacksquare $k = 0.01$, \bullet $k = 1.0$, \blacktriangle $k = 0.3$, \blacktriangledown $k = 0.5$, \blacklozenge $k = 1.0$, \blacktriangleleft $k = 2.0$, \blacktriangleright $k = 4.0$, \bullet $k = 10.0$.

Table 1 Material property of the individual constituent

Constituent (property)	E (GPa)	ρ (kg/m ³)	ν	$\alpha(10^{-6}/^{\circ}\text{C})$
Aluminium (metal)	70	2,707	0.3	23.5
Alumina (ceramic)	380	3,800	0.22	12.66
Zirconia (ceramic)	151	5,700	0.31	12.766

Table 2 Configuration in different sandwich FGM panel symmetry

Symmetry	h_0	h_1	h_2	h_3
1-0-1	$-h/2$	0	0	$h/2$
1-1-1	$-h/2$	$-h/6$	$h/6$	$h/2$
1-2-1	$-h/2$	$-h/4$	$h/4$	$h/2$
2-1-2	$-h/2$	$-h/10$	$h/10$	$h/2$
1-2-2	$-h/2$	$-3h/10$	$h/10$	$h/2$

The combination of free (F) simply-supported (S) and clamped (C) supports (SSSS, HHHH, CCCC, SCSC and CFCF) as mentioned in the following lines have been utilised as constraint conditions for solving the present boundary value problem and obtaining the free vibration responses. The ambient temperature (300 K) is considered as the reference temperature and the uniform thermal load is applied with respect to the reference temperature.

a Free (F)

$$x = 0, a; y = 0, b \quad u_{x0} = u_{y0} = u_{z0} = \varphi_x = \varphi_y = \psi_x = \psi_y = \theta_x = \theta_y \neq 0$$

b Simply supported (S)

$$x = 0, a \quad u_{y0} = u_{z0} = \varphi_y = \psi_y = \theta_y = 0; y = 0, b \quad u_{x0} = u_{z0} = \varphi_x = \psi_x = \theta_x = 0$$

c Clamped (C)

$$x = 0, a; y = 0, b \quad u_{x0} = u_{y0} = u_{z0} = \varphi_x = \varphi_y = \psi_x = \psi_y = \theta_x = \theta_y = 0$$

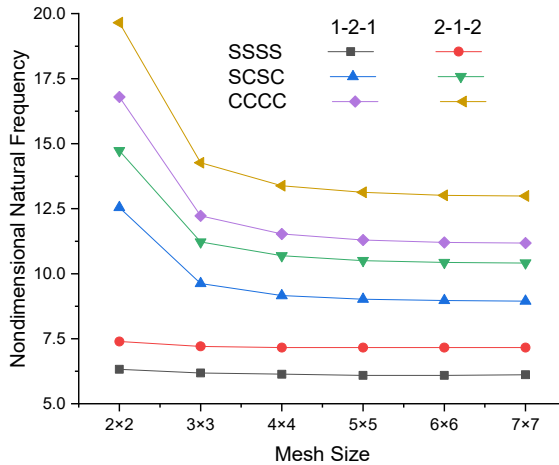
d Hinged

$$x = 0, a \quad u_{x0} = u_{y0} = u_{z0} = \varphi_y = \psi_y = \theta_y = 0; y = 0, b \quad u_{x0} = u_{y0} = u_{z0} = \varphi_x = \psi_x = \theta_x = 0.$$

3.1 Convergence test

In an intention to reduce the solve time and ensure accurate capture of the system behaviour by the present model, the convergence test has been performed. The sandwich panels under three different support conditions (SSSS, SCSC, CCCC) with top as well as bottom surface consisting of FGM (silicon nitride-stainless steel) and the core as pure metal are considered to determine the non-dimensional natural frequencies considering the geometrical ($h = 0.025$ m, $a = 0.2$ m, $a/b = 1$, $a/h = 10$, $R/a = 10$ and $k = 2$) and temperature dependent material properties as used by Huang and Shen (2004). The free vibration responses are computed for various mesh refinement considering sandwich FGM type of 1-2-1 and 2-1-2 configurations and portrayed in Figure 4. According to the results of the convergence test, a (6×6) mesh has been found suitable and utilised for further calculation of the natural frequencies using the present model.

Figure 4 Convergence test for the non-dimensional natural frequency (see online version for colours)

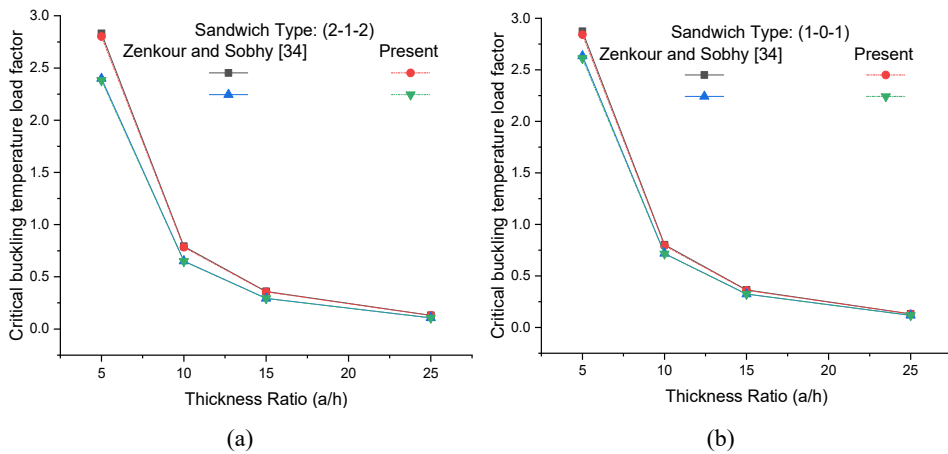


3.2 Validation

In the present analysis, the temperature load to which the FGMS structures are exposed is determined by computing the critical buckling temperature load factor [using equation (27)] for each combination of geometrical parameters and constraint conditions. Therefore, while demonstrating the efficacy of the present model, first the critical buckling temperature load factor is calculated for diverse (a/h) values and compared with the analytical values of Zenkour and Sobhy (2010). From the results presented in

Figure 5, it is confirmed that the values are well matching with the values of Zenkour and Sobhy (2010) for different temperature conditions as well as FGMS symmetry (1-0-1 and 2-1-2). Further, the examples pertaining to the natural frequencies of FGM (silicon nitride-stainless steel) sandwich panel under different uniform thermal loading ($T = 300$ K, 400 K and 600 K) as available in Pandey and Pradyumna (2015) and Huang and Shen (2004) are solved using the geometrical and material properties in tune with the individual references and the corresponding results are shown in Figures 6(a) and 6(b), respectively. It can be clearly observed that the presently acquired critical buckling temperature load factor values as well as the non-dimensional mode 1 and mode 2 fundamental frequencies over various k values are establishing excellent agreement with the existing reference values under uniform thermal loading conditions. Therefore, it can be concluded that the current model yields correct and valid results.

Figure 5 Validation of critical buckling temperature load factor with analytical values (Zenkour and Sobhy, 2010) under uniform temperature loading (a) 2-1-2, and (b) 1-0-1 FGMS plate (see online version for colours)



3.3 Parametric study

It is well known that the natural frequency is the basic design property for assessing the stress and deformation of any structure and therefore, it is vital for the analysis of different parameters influencing it. Moreover, the effect of thermal environment has a significant influence on the stiffness of the material due to the fact that the different geometrical parameters are affected by the change in temperature, and they influence the final behaviour of the structure. This segment puts emphasis on the investigation on the influence of diverse design variables such as curvature, power-law index, support conditions, thickness ratio, aspect ratio and sandwich FGM symmetry types alongside constituent material on the natural frequency of hardcore sandwich FGM curved shell panel under the influence of uniform thermal environment by the use of the present numerical model. Various numerical illustrations are solved for cylindrical, spherical, hyperbolic, elliptical, and flat panel geometries having different sandwich symmetry type such as 1-0-1, 1-1-1, 1-2-1, 2-1-2 and 1-2-2 under the influence of two different uniform

temperatures fields ($T = 400$ K and $T = 600$ K) with the help of the present higher-order FE model and the results are discussed in detail.

Figure 6 Validation of nondimensional frequency responses of FGM sandwich plate with numerical solutions Pandey and Pradyumna (2015) under different uniform thermal loading (a) $T = 300$ K, (b) $T = 400$ K, and (c) $T = 600$ K, and analytical solutions Huang and Shen (2004) under uniform thermal loading (d) $T = 300$ K, (e) $T = 400$ K and, (f) $T = 600$ K (see online version for colours)

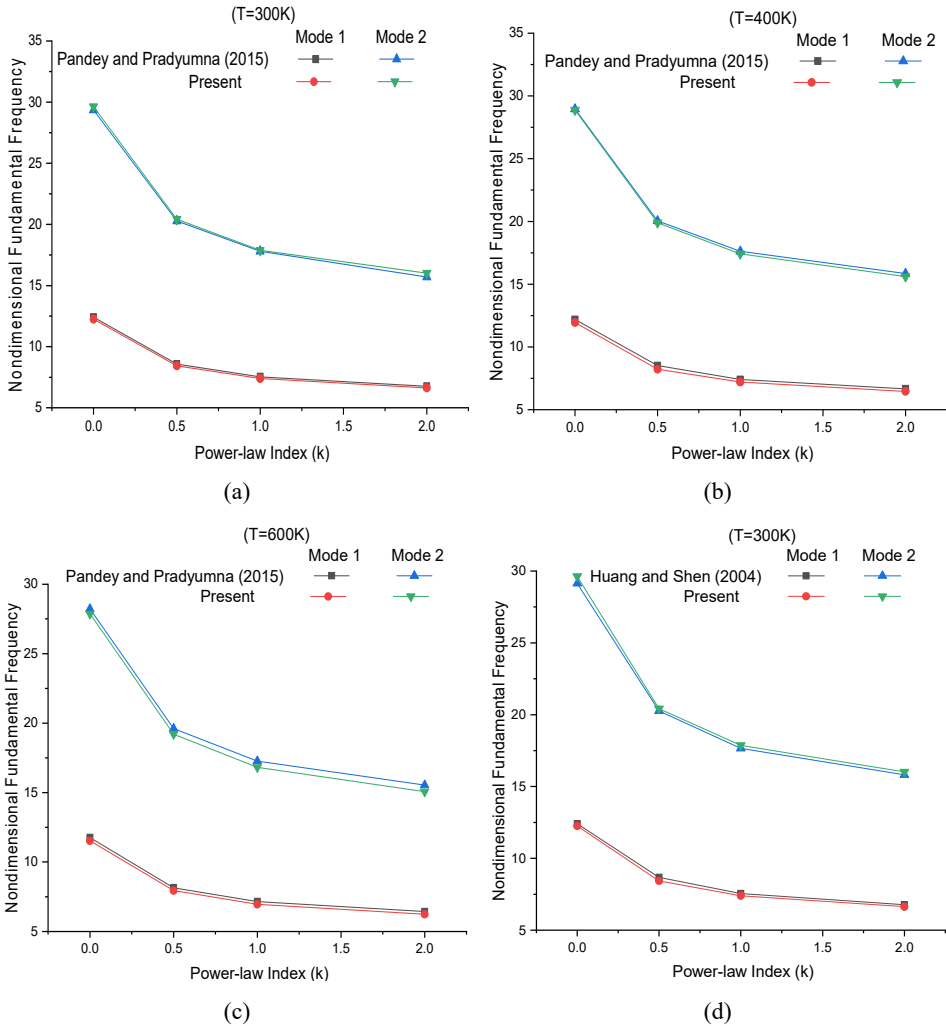
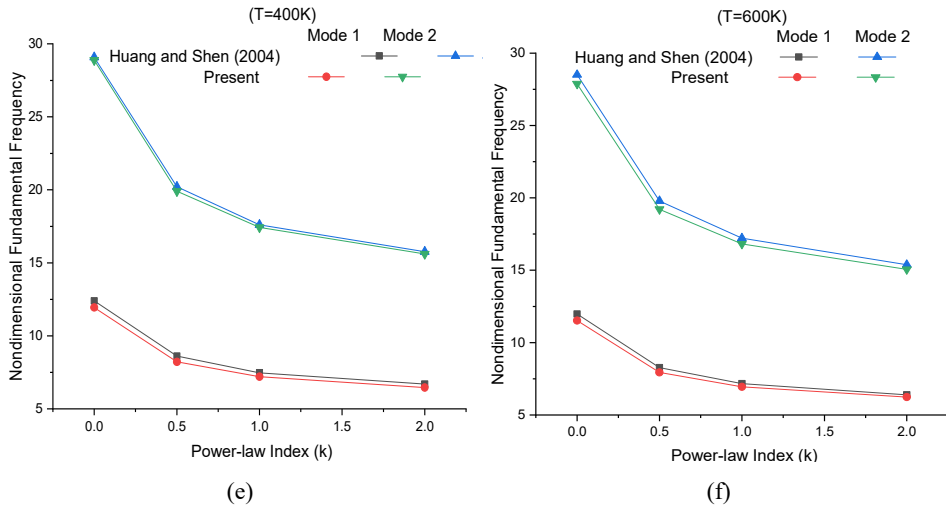


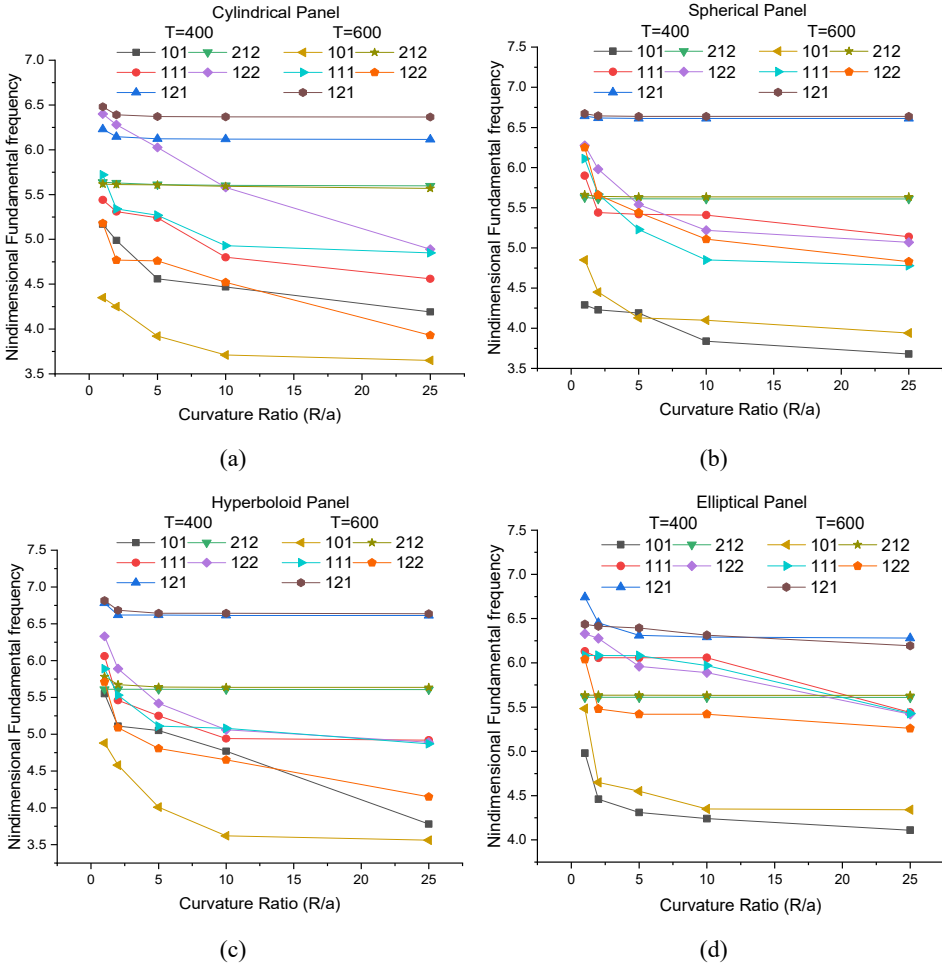
Figure 6 Validation of nondimensional frequency responses of FGM sandwich plate with numerical solutions Pandey and Pradyumna (2015) under different uniform thermal loading (a) $T = 300\text{K}$, (b) $T = 400\text{K}$, and (c) $T = 600\text{K}$, and analytical solutions Huang and Shen (2004) under uniform thermal loading (d) $T = 300\text{K}$, (e) $T = 400\text{K}$ and, (f) $T = 600\text{K}$ (continue) (see online version for colours)



3.3.1 Effect of curvature ratio

Before all else, the curvature effect ($R/a = 1, 2, 5, 10$ and 25) on the natural frequency of doubly curved hard-core sandwich FGM shell panels under mixed support condition (SCSC) under the influence of uniform temperature load ($T = 400\text{ K}$ and 600 K) along the thickness is examined. The computed results for the increasing (R/a) values are represented in Figure 7. It can be clearly seen that the frequency value decreases with increasing curvature ratio values for each of the geometry panels irrespective of the temperature loads. This is due to the fact that in the present numerical scheme, keeping all other geometrical parameters constant, the panel tends to flatten with increasing curvature ratio that results in reduced stiffness and thus, decreasing the value of natural frequency. Further, it is also noticed that the sandwich type 1-0-1 and 1-2-1 exhibit the lowest and the highest frequency values disregarding the geometry of the sandwich structure. This may be attributed to the fact that, in 1-0-1 type hard-core sandwich there is less proportion of ceramic as compared to 1-2-1 symmetric sandwich type in which the proportion of ceramic is double in comparison to the metal on the upper and lower face. The graphs also put emphasis on the fact that as the proportion of ceramic goes on increasing in comparison to metal, a particular sandwich type exhibits lower frequency at $T = 400\text{ K}$ than at $T = 600\text{ K}$ as the ceramic is more thermal resistant as compared to metal. Additionally, it is worthy to mention that the percentage increase in the natural frequency at higher temperature ($T = 600\text{ K}$) is more for lower curvature in comparison to that for the higher curvature, that signifies the usefulness of curved structures under hostile environment.

Figure 7 Impact of curvature ratio on non-dimensional fundamental frequency of hardcore FGMS panel in thermal environment, (a) cylindrical (b) spherical (c) hyperboloid (d) elliptical (see online version for colours)



3.3.2 Effect of power-law index

Simply supported flat and doubly curved hardcore sandwich panels ($a/h = 25$ and $R/a = 20$) are now studied to examine the behaviour of natural frequency under the influence of different power-law index (k) values (0.5, 1, 2, 5 and 10). The influence of increasing k values on the natural frequency for different sandwich types under consideration are portrayed in Figure 8. From the results, it is observed that the value of fundamental frequency decreases unvaryingly with increase in power-law value for all geometries under different thermal environment. More precisely it is perceived from the graph that the fundamental frequency values are highest at lower values of power-law index justifying the fact that the materials are stiffer at those particular values in comparison to the higher ones. However, the non-dimensional frequency values are higher at temperature $T = 400$ K for sandwich type 1-1-1, 2-1-2 and 1-2-2 in comparison

the corresponding values at temperature $T = 600$. Out of all the geometrical panels the overall natural frequency for all the sandwich type in flat panels is much lower which is due to the fact that flat panels are less stiff and hence the natural frequency is less in comparison to other geometrical panels under the influence of different thermal loading conditions.

3.3.3 Effect of thickness ratio

Now, all sides clamped hardcore sandwich FGM single and doubly curved panels ($a/b = 1$ and $R/a = 20$) are examined to bring out the effect of thickness ratio (a/h) on the fundamental frequency parameter. It is important to mention here that, for the present analysis purpose, the overall thickness (h) of the sandwich structure is considered to be constant while the length (a) is varied so as to attain the five different values of thickness ratios (25, 50, 75, 100, 125). The influence of (a/h) values on the natural frequency under the effect of thermal environment is examined for different sandwich symmetry types and reported in Figure 9. It is observed that the natural frequency has an increasing trend versus the thickness ratio irrespective of the geometry of the sandwich structure under consideration. This is because in the present model, with increasing (a/h) values the span of the structure decreases for a continual overall thickness which in turn improves the overall stiffness and results in increasing fundamental frequency. Figure 9 also puts emphasis on the point that for a particular geometrical pattern, the natural frequency for all the sandwich type has greater value at temperature $T = 600$ K than the frequencies at temperature $T = 400$ K. This also clarifies the fact that the graded structures tend to become stiffer at higher temperatures and thus are thermal resistant in extreme service conditions. Also, the unsymmetric sandwich type (1-2-2) exhibits lower values of frequency in comparison to the symmetric sandwich types justifying the fact that the sandwich FGM with unsymmetric configuration is less stiff in comparison to the symmetric counter parts under hostile environment.

3.3.4 Effect of aspect ratio

In order to investigate the effect of aspect (side-to-width) ratio, the side span (a) is considered as constant (as per a constant overall thickness h and thickness ratio value) and the width b is varied to attain diverse aspect ratios. The non-dimensional free vibration responses of cantilever (CFFF) hardcore sandwich FGM flat as well as curved panels ($a/h = 20$ and $R/a = 10$) of different sandwich symmetries under two different temperature loading are computed for diverse (a/b) values (0.5, 1.0, 1.5, 2.0 and 2.5) and shown in Figure 10. It is appraised from the results that the fundamental frequencies follow a decreasing trend with the increasing value of aspect ratio for all the five geometrical panels irrespective of intensity of temperature loading. Further, upon comparing the natural frequencies corresponding to both the temperatures, it is observed that the values are lower under lesser temperature loading ($T = 400$ K) in accordance with the fact that the stiffness of the hardcore FGM structure increases with rise in temperature irrespective of the panel geometry. However, the natural frequency when compared with the lowest value of aspect ratio shows a greater percentage of increase in both hyperboloid and flat panels thus making it convincible that at lower values of aspect ratio the aforesaid geometrical panels are stiffer in comparison to the other types of geometries.

Figure 8 Impact of power-law index on non-dimensional fundamental frequency of hardcore FGMS panel in thermal environment, (a) cylindrical (b) spherical (c) hyperboloid (d) elliptical (e) flat (see online version for colours)

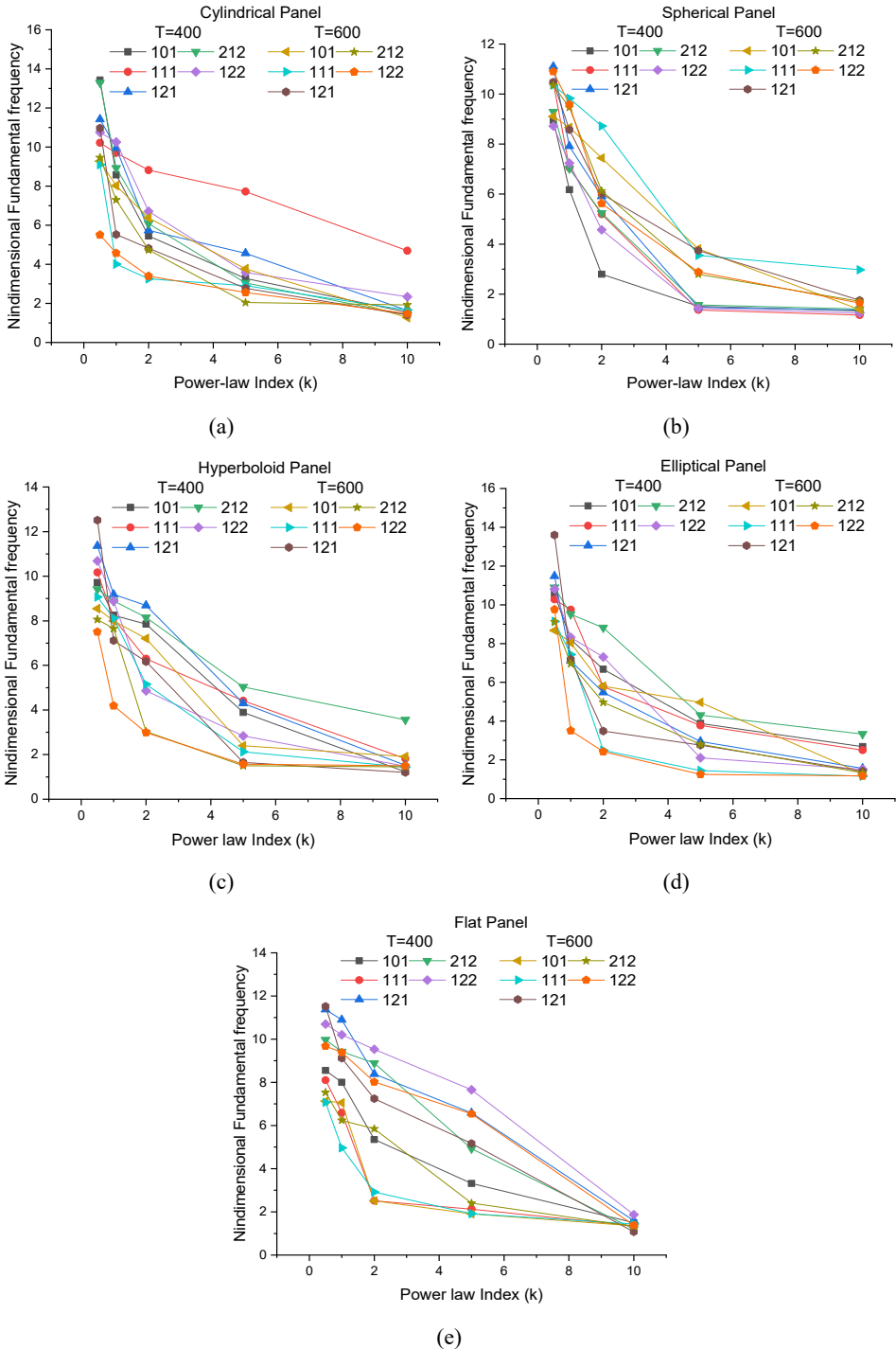


Figure 9 Impact of thickness ratio on non-dimensional fundamental frequency of hardcore FGMS panel in thermal environment, (a) cylindrical (b) spherical (c) hyperboloid (d) elliptical (e) flat (see online version for colours)

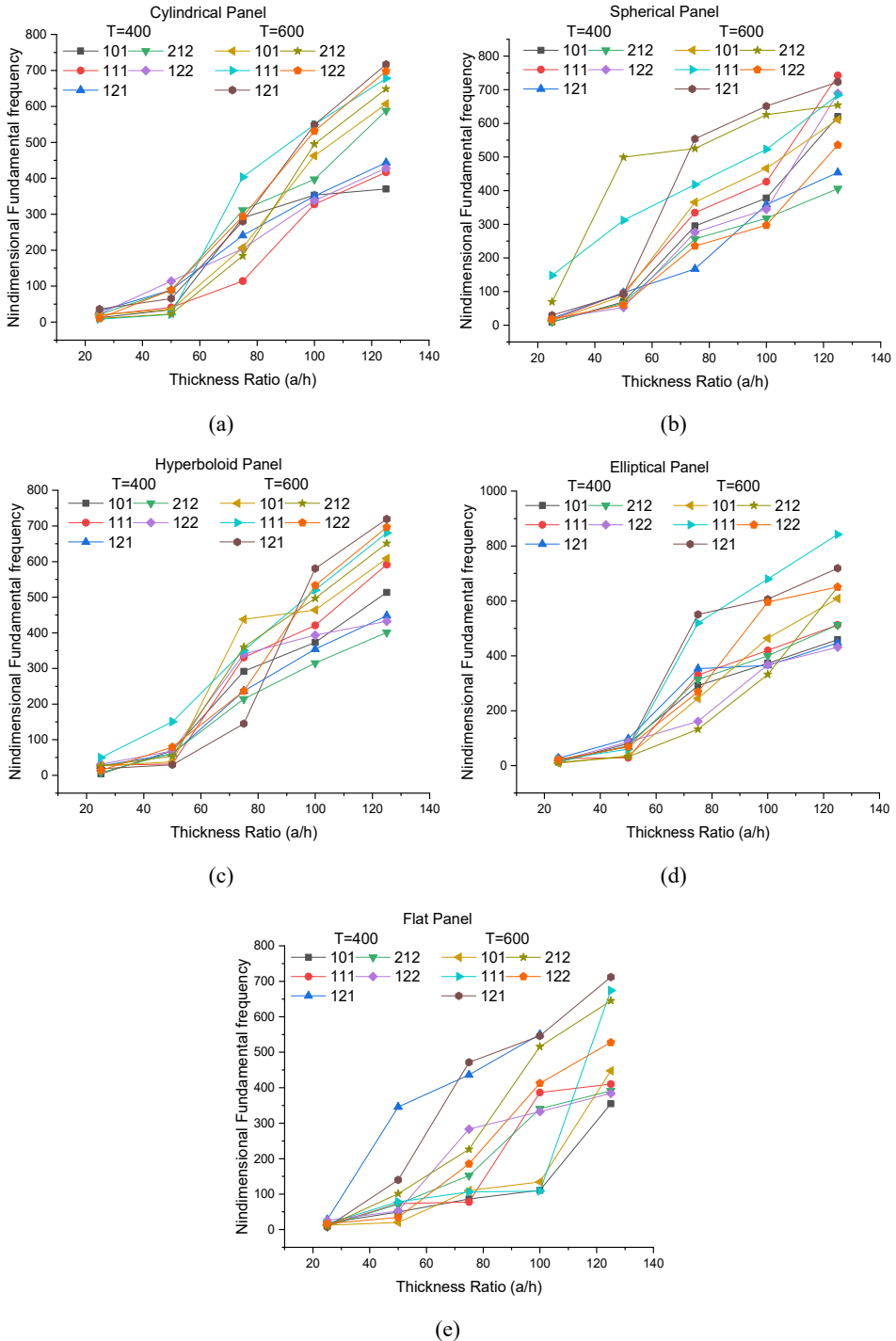


Figure 10 Impact of aspect ratio on non-dimensional fundamental frequency of hardcore FGMS panel in thermal environment, (a) cylindrical (b) spherical (c) hyperboloid (d) elliptical (e) flat (see online version for colours)

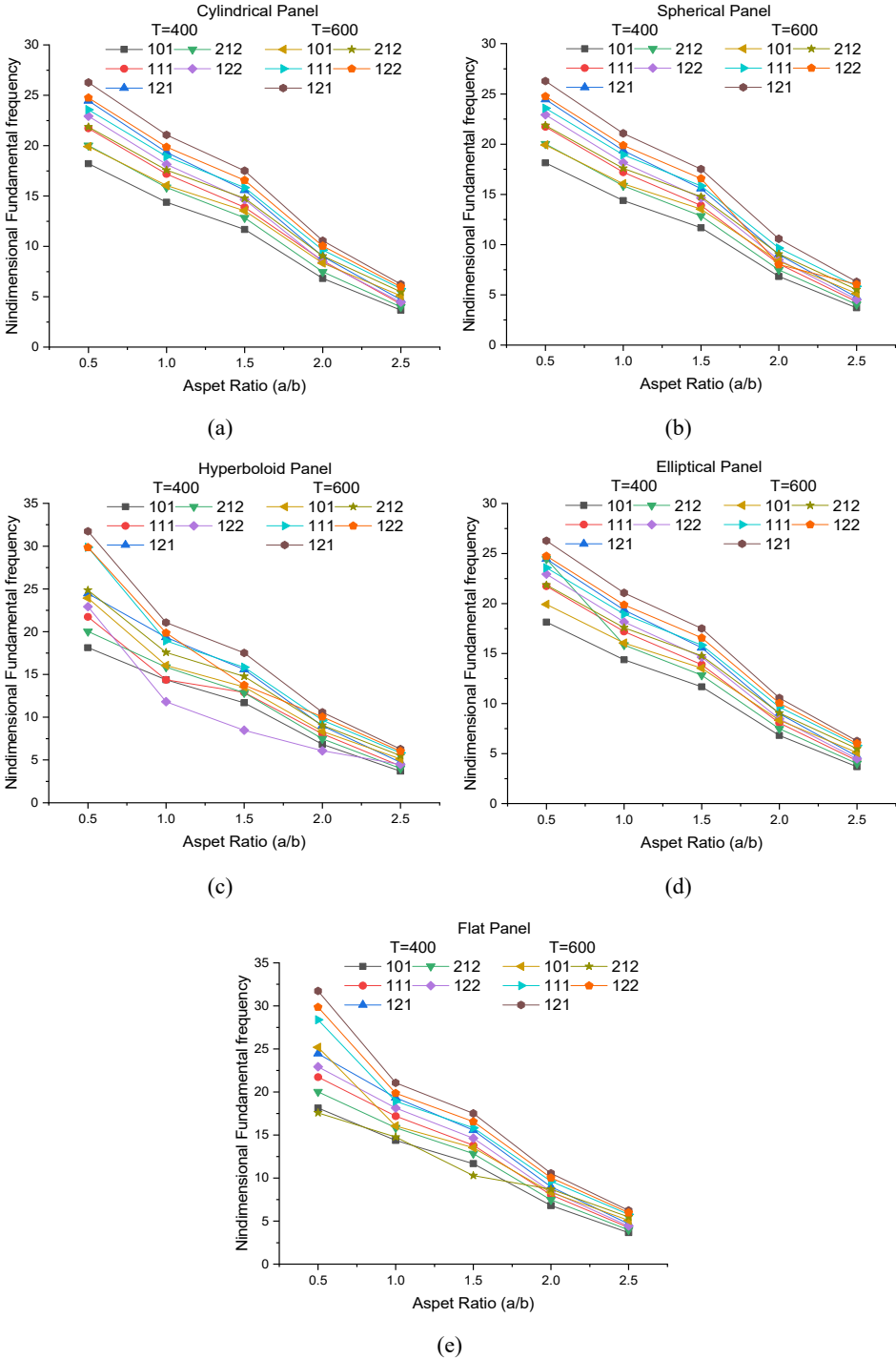
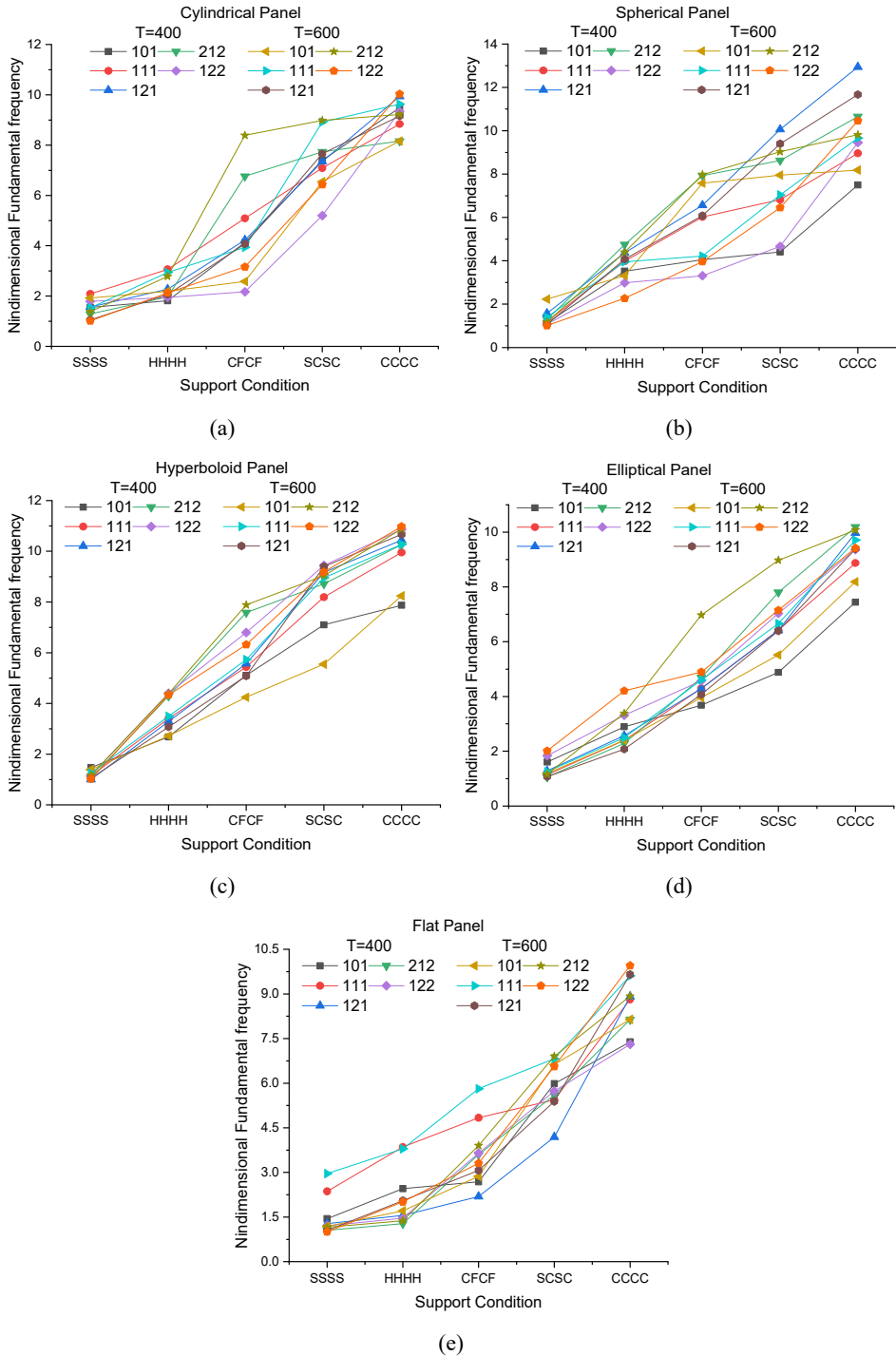


Figure 11 Impact of constraint conditions at support on non-dimensional fundamental frequency of hardcore FGMS panel in thermal environment: (a) cylindrical, (b) spherical, (c) hyperboloid, (d) elliptical (e) flat (see online version for colours)



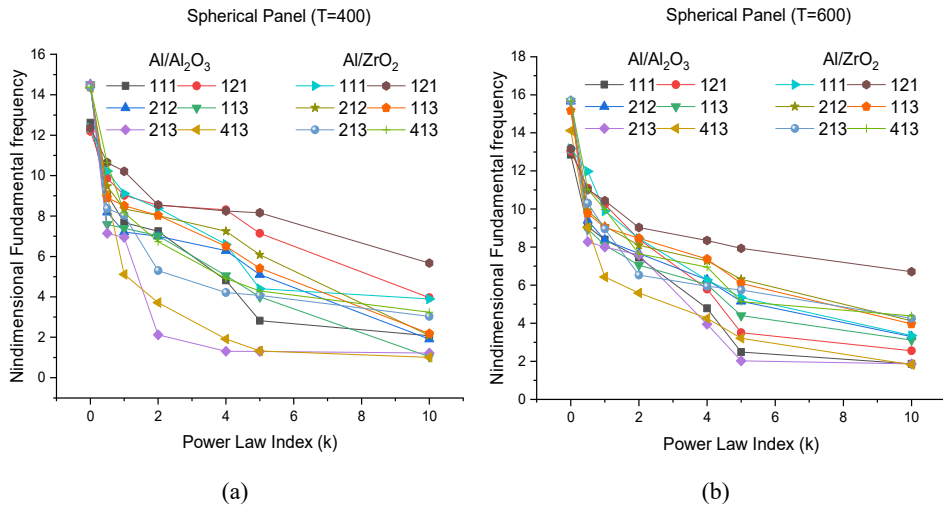
3.3.5 *Effect of support condition*

As the effect of support condition is an important parameter in determining the stiffness of a structure, it becomes essential to understand the behaviour of the structure under the influence of various boundary conditions for justifying its utility for a particular service. The thermoelastic fundamental frequencies of hardcore sandwich FGM panels ($R/a = a/h = 10$) with different sandwich symmetries under various support conditions such as SSSS, CCCC, SCSC CFCF and HHHH are computed for all the geometrical panels and depicted in Figure 11. It is observed that as the number of constraints goes on increasing the stiffness of the sandwich FGM panel goes on increasing thus giving an increasing trend of non-dimensional frequency irrespective of panel geometry. A weird pattern can be observed from the graphical representation that the sandwich type which are having lesser proportion of ceramic such as 1-0-1 as compared to larger proportion of ceramic (1-2-1 and 1-2-2) exhibit lower frequency at higher temperatures ($T = 600$ K) as compared to lower temperatures ($T = 400$ K) justifying the fact that ceramic is more thermal resistant alongside stiffer for increasing number of constraints. Also, it is interesting to note that the cylindrical and spherical panel have similar pattern of behaviour in terms of the fundamental frequency under the different constraint conditions considered when compared with the elliptical and hyperboloid panels, but an entirely different pattern of behaviour is observed in case of flat panel which has lesser stiffness as compared to curved panels under different thermal environment.

3.3.6 *Effect of sandwich configuration*

Eventually the effect of sandwich symmetry type on the non-dimensional frequency for simply supported spherical panel under the influence of different temperature loading is studied. For the present analysis, two different combinations graded structures namely aluminium-alumina ($\text{Al}/\text{Al}_2\text{O}_3$) and aluminium-zirconia (Al/ZrO_2) are considered. Different symmetric (1-1-1, 1-2-1 and 2-1-2) and unsymmetric (1-1-3, 2-1-3 and 4-1-3) sandwich configurations of sandwich FGM square panels ($R/a = 5$, $a/h = 10$ and $a/b = 1$) with increasing power-law index ($k = 0, 0.5, 1, 2, 4, 5$ and 10) vales have been utilised for the computation purpose. From the results provided in Figure 12, it is observed that the fundamental frequencies exhibit a decreasing pattern with increasing value of power-law index for both aluminium-alumina and aluminium-zirconia strongly agreeing with the fact that the stiffness of the said material goes on decreasing with increasing power-law value. Further, it is also observed that the unsymmetric sandwich types exhibit higher frequency when compared with the symmetric sandwich types which may be attributed to the greater stiffness associated with the unsymmetric configurations under consideration. Upon comparing the behaviour of aluminium-zirconia with aluminium-alumina, it is also found that the sandwich type with aluminium-zirconia combination has the higher frequency thus, it is confirmed that the aluminium-zirconia panels are much stiffer than other panels. Moreover, it is also found that there is a marginal increase in the value of the fundamental frequency at higher temperature ($T = 600$ K) for both the combinations of constituent materials.

Figure 12 Impact of sandwich symmetry type on non-dimensional fundamental frequency of hardcore FGMS panel in thermal environment (a) Al/Al₂O₃ and (b) Al/ZrO₂ FGMS shell panel (see online version for colours)



4 Conclusions

The thermoelastic fundamental frequencies of functionally graded hardcore sandwich single and doubly curved panel (flat, hyperboloid, elliptical, spherical, and cylindrical) structures are computed numerically. The upper and the bottom layer of the sandwich structure are assumed to be made up of isotropic materials whose material properties are graded smoothly along the thickness towards the core which is made up of pure ceramic. In attempt to attain greater degree of accuracy alongside simplicity, the FE formulation is derived by utilising a higher-order shell theory which is devoid of shear correction factor and discretised (for the first time) by employing a nine-nodded isoparametric Lagrangian element replicating full quadratic interpolation function. The convergence and validation test indicated excellent convergence rate as well as efficacy of the present numerical scheme in terms of computing critical buckling temperature load and the fundamental frequency of vibration in thermal environment for the functionally graded sandwich structure. A detailed numerical study is performed to investigate the influence of various design parameters like curvature ratio, type of geometry, aspect ratio, power-law index, support conditions and the symmetry configurations on the natural frequency of hardcore graded sandwich panel structure under the influence of uniform thermal loading. It is observed that the natural frequency has a decreasing trend for increasing value of curvature ratio, power-law index, aspect ratio and increases with increasing number of constraints at the support and the thickness ratio values irrespective of the geometry as well as temperature load. For a particular geometrical pattern, the natural frequency values are lower at higher temperature for all the sandwich configurations under consideration. Moreover, the unsymmetric sandwich types exhibit lower values of frequency in comparison to the symmetric sandwich types. Also, the sandwich structure

with aluminium-zirconia combination exhibits greater frequency in comparison to aluminium-alumina combination.

Acknowledgements

This work is supported by the Department of Science and Technology, Government of India under Start-up Research Grant (SRG) via Reference no. (SERB/F7721/2019-20, dated 17 December 2020).

References

- Aghababaei, R. and Reddy, J.N. (2009) 'Nonlocal third-order shear deformation plate theory with application to bending and vibration of plates', *Journal of Sound and Vibration*, Vol. 326, No. 1, pp.277–289.
- Attia, A., Tounsi, A., Bedia, E.A.A. and Mahmoud, S.R. (2015) 'Free vibration analysis of functionally graded plates with temperature-dependent properties using various four variable refined plate theories', *Steel and Composite Structures*, Vol. 18, No. 1, pp.187–212.
- Belarbi, M.O., Garg, A., Houari, M.S.A., Hirane, H., Tounsi, A. and Chalak, H.D. (2021) 'A three-unknown refined shear beam element model for buckling analysis of functionally graded curved sandwich beams', *Engineering with Computers*, July [online] <https://doi.org/10.1007/s00366-021-01452-1>.
- Berghouti, H., Bedia, E.A.A., Benkhedda, A. and Tounsi, A. (2019) 'Vibration analysis of nonlocal porous nanobeams made of functionally graded material', *Advances in Nano Research*, Vol. 7, No. 5, pp.351–364 [online] <https://doi.org/10.12989/anr.2019.7.5.351>.
- Burlayenko, V.N., Sadowski, T. and Dimitrova, S. (2019) 'Three-dimensional free vibration analysis of thermally loaded FGM sandwich plates', *Materials*, Vol. 12, No. 15, p.2377.
- Chaabane, L.A., Bourada, F., Sekkal, M., Zerouati, S., Zaoui, F.Z., Tounsi, A., Derras, A., Bousahla, A.A. and Tounsi, A. (2019) 'Analytical study of bending and free vibration responses of functionally graded beams resting on elastic foundation', *Structural Engineering and Mechanics*, Vol. 71, No. 2, pp.185–196.
- Cook, R.D., Plesha, M. and Witt, R.J. (2007) *Concepts and Applications of Finite Element Analysis*, 4th ed., John Wiley & Sons, Singapore.
- Daikh, A.A. (2019) 'Temperature dependent vibration analysis of functionally graded sandwich plates resting on Winkler/Pasternak/Kerr foundation', *Materials Research Express*, Vol. 6, No. 6, p.065702 [online] <https://doi.org/10.1088/2053-1591/ab097b>.
- Gupta, A. and Talha, M. (2018) 'Influence of porosity on the flexural and free vibration responses of functionally graded plates in thermal environment', *International Journal of Structural Stability and Dynamics*, Vol. 18, No. 1, p.1850013.
- Hirane, H., Belarbi, M.O., Houari, M.S.A. and Tounsi, A. (2021) 'On the layerwise finite element formulation for static and free vibration analysis of functionally graded sandwich plates', *Engineering with Computers*, January [online] <https://doi.org/10.1007/s00366-020-01250-1>.
- Huang, X.L. and Shen, H.S. (2004) 'Nonlinear vibration and dynamic response of functionally graded plates in thermal environments', *International Journal of Solids and Structures*, Vol. 41, No. 9, pp.2403–2427.
- Joseph, S.V. and Mohanty, S.C. (2019) 'Temperature effects on buckling and vibration characteristics of sandwich plate with viscoelastic core and functionally graded material constraining layer', *Journal of Sandwich Structures & Materials*, Vol. 21, No. 4, pp.1557–1577.

- Kant, T. and Swaminathan, K. (2002) 'Analytical solutions for the static analysis of laminated composite and sandwich plates based on a higher order refined theory', *Composite Structures*, Vol. 56, No. 4, pp.329–344.
- Karami, B., Janghorban, M. and Tounsi, A. (2019a) 'Galerkin's approach for buckling analysis of functionally graded anisotropic nanoplates/different boundary conditions', *Engineering with Computers*, Vol. 35, No. 4, pp.1297–1316.
- Karami, B., Janghorban, M. and Tounsi, A. (2019b) 'On pre-stressed functionally graded anisotropic nanoshell in magnetic field', *Journal of the Brazilian Society of Mechanical Sciences and Engineering*, Vol. 41, No. 11, p.495.
- Khalili, S.M.R. and Mohammadi, Y. (2012) 'Free vibration analysis of sandwich plates with functionally graded face sheets and temperature-dependent material properties: a new approach', *European Journal of Mechanics - A/Solids*, Vol. 35, pp.61–74.
- Kolahchi, R. (2017) 'A comparative study on the bending, vibration and buckling of viscoelastic sandwich nano-plates based on different nonlocal theories using DC, HDQ and DQ methods', *Aerospace Science and Technology*, Vol. 66, pp.235–248.
- Li, Q., Iu, V.P. and Kou, K.P. (2008) 'Three-dimensional vibration analysis of functionally graded material sandwich plates', *Journal of Sound and Vibration*, Vol. 311, No. 1, pp.498–515.
- Mahapatra, T.R., Kar, V.R., Panda, S.K. and Mehar, K. (2017) 'Nonlinear thermoelastic deflection of temperature-dependent FGM curved shallow shell under nonlinear thermal loading', *Journal of Thermal Stresses*, Vol. 40, No. 9, pp.1184–1199.
- Mahapatra, T.R., Panda, S.K. and Kar, V.R. (2015) 'Geometrically nonlinear flexural analysis of hygro-thermo-elastic laminated composite doubly curved shell panel', *International Journal of Mechanics and Materials in Design*, Vol. 12, No. 2, pp.153–171.
- Mahmoudi, A., Benyoucef, S., Tounsi, A., Benachour, A., Bedia, E.A.A. and Mahmoud, S.R. (2019) 'A refined quasi-3D shear deformation theory for thermo-mechanical behavior of functionally graded sandwich plates on elastic foundations', *Journal of Sandwich Structures & Materials*, Vol. 21, No. 6, pp.1906–1929.
- Mantari, J.L. and Monge, J.C. (2016) 'Buckling, free vibration and bending analysis of functionally graded sandwich plates based on an optimized hyperbolic unified formulation', *International Journal of Mechanical Sciences*, Vol. 119, pp.170–186.
- Mouffoki, A., Aicha, B., Houari, M.S.A., Abdelhakim, K., Tounsi, A. and Bedia, E.S.A. (2019) 'Thermo-mechanical vibration analysis of non-local refined trigonometric shear deformable FG beams', *International Journal of Hydromechanics*, Vol. 2, No. 1, pp.54–62.
- Natarajan, S. and Manickam, G. (2012) 'Bending and vibration of functionally graded material sandwich plates using an accurate theory', *Finite Elements in Analysis and Design*, Vol. 57, pp.32–42.
- Pandey, S. and Pradyumna, S. (2015) 'A layerwise finite element formulation for free vibration analysis of functionally graded sandwich shells', *Composite Structures*, Vol. 133, pp.438–450.
- Pandey, S. and Pradyumna, S. (2017) 'A finite element formulation for thermally induced vibrations of functionally graded material sandwich plates and shell panels', *Composite Structures*, Vol. 160, pp.877–886.
- Phu, K.V., Bich, D.H. and Doan, L.X. (2021) 'Nonlinear forced vibration and dynamic buckling analysis for functionally graded cylindrical shells with variable thickness subjected to mechanical load', *Iranian Journal of Science and Technology, Transactions of Mechanical Engineering*, March [online] <https://doi.org/10.1007/s40997-021-00429-1>.
- Rahmani, M.C., Kaci, A., Bousahla, A.A., Bourada, F., Tounsi, A., Bedia, E.A.A., Mahmoud, S.R., Benrahou, K.H. and Tounsi, A. (2020) 'Influence of boundary conditions on the bending and free vibration behavior of FGM sandwich plates using a four-unknown refined integral plate theory', *Computers and Concrete*, Vol. 25, No. 3, pp.225–244.
- Srividhya, S., Kumar, B., Gupta, R.K. and Rajagopal, A. (2019) 'Nonlinear analysis of FGM plates using generalised higher order shear deformation theory', *Int. J. Materials and Structural Integrity*, Vol. 13, Nos. 1/2/3, pp.3–15.

- Tounsi, A., Houari, M.S.A. and Bessaim, A. (2016) 'A new 3-unknowns non-polynomial plate theory for buckling and vibration of functionally graded sandwich plate', *Structural Engineering and Mechanics*, Vol. 60, No. 4, pp.547–565.
- Vinh, P.V. and Tounsi, A. (2021) 'The role of spatial variation of the nonlocal parameter on the free vibration of functionally graded sandwich nanoplates', *Engineering with Computers*, July [online] <https://doi.org/10.1007/s00366-021-01475-8>.
- Zenkour, A.M. (2005) 'A comprehensive analysis of functionally graded sandwich plates: part 1 – deflection and stresses', *International Journal of Solids and Structures*, Vol. 42, No. 18, pp.5224–5242.
- Zenkour, A.M. (2013) 'Bending analysis of functionally graded sandwich plates using a simple four-unknown shear and normal deformations theory', *Journal of Sandwich Structures & Materials*, Vol. 15, No. 6, pp.629–656.
- Zenkour, A.M. and Sobhy, M. (2010) 'Thermal buckling of various types of FGM sandwich plates', *Composite Structures*, Vol. 93, No. 1, pp.93–102.
- Ziou, H., Guenfoud, H. and Guenfoud, M. (2016) 'Numerical modelling of a Timoshenko FGM beam using the finite element method', *Int. J. Structural Engineering*, Vol. 7, No. 3, pp.239–261.